

# Structure of low and high spin states in $^{112}\text{Sb}$ in interacting boson fermion fermion model

A.K. Singh

Department of Physics, University College of Science, University of Calcutta, 92, Acharya Prafulla Chandra Road, Calcutta 700 009, India

Received: 23 December 1997 / Revised version: 30 April 1998

Communicated by P. Schuck

**Abstract.** In this paper, properties of the low and the high spin states in  $^{112}\text{Sb}$  have been studied in the framework of Interacting Boson Fermion Fermion Model. A surface delta plus spin-spin type of interaction has been taken as the residual interaction between the odd neutron and the odd proton. Energy values, magnetic moments of the ground state and the isomeric  $8^-$  state, E2/M1 mixing ratios of some of the low-lying transitions and  $\log ft$  values for the Gamow-Teller transitions in  $^{112}\text{Sb} \rightarrow ^{112}\text{Sn}$  and  $^{111}\text{Sb} \rightarrow ^{111}\text{Sn}$  decay have been calculated and are compared with the experimental results. The band based on the configuration  $\pi g_{9/2}^{-1} \pi g_{7/2}^2 \otimes \nu h_{11/2}$  is obtained in this calculation by coupling the proton in the  $g_{9/2}$  and the neutron in the  $h_{11/2}$  orbital to the deformed band of  $^{110}\text{Sn}$ . The B(M1)/B(E2) ratios and branching ratios for the transitions in this band have also been calculated and compared with the experimental results.

**PACS.** 21.60.Fw Models based on group theory – 21.10.Ky Electromagnetic moments – 21.10.Tg Lifetimes – 23.40.Hc Relation with nuclear matrix elements and nuclear structure – 27.60.+j  $90 \leq A \leq 149$

## 1 Introduction

Tin and antimony nuclei have been a testing ground for models and methods in nuclear structure calculations [1] and are ideal for studying the behaviour of the different excitation mechanisms present in spherical nuclei. Reasonable successes have been achieved in describing the low lying states in even-even and odd-mass nuclei in terms of collective vibration and the particle-vibration coupling model, respectively [2,3]. However, the observation of a rotational band on the excited  $0^+$  state in even-even  $^{112-118}\text{Sn}$  [4] nuclei, suggests the onset of deformation in these nuclei at a higher excitation energy. Recently, rotational bands of similar character have also been observed in lighter even Sn isotopes down to  $^{106,108}\text{Sn}$  nuclei [5–7]. The origin of these states lies in the particle excitations across the  $Z = 50$  shell. The coexistence of these structures largely modify the decay patterns, transition probabilities and branching ratios, etc., and makes the structure more complex. A configuration mixing calculation based on IBM-2 model in the even-even Sn isotopes nicely reproduces these features [8]. Deformed structures with similar origin have also been observed in the form of rotational bands based on the  $\pi g_{9/2}^{-2} \pi g_{7/2}^2 \otimes \nu h_{11/2}$  configuration [9, 10] in odd Sn isotopes and on the  $\pi g_{9/2}^{-2} \pi g_{7/2}^2 \otimes \pi h_{11/2}$  and  $\pi g_{9/2}^{-1} \pi g_{7/2}^2$  configurations in odd-mass Sb nuclei [11–18].

The studies of odd-odd nuclei are limited due to the necessity of considering a large configuration space to describe the complex structure. However, the study of odd-odd nucleus is important and offers an opportunity to investigate the residual interaction between the nucleons. This can be studied best in nuclei near doubly closed shell. The nuclei near singly closed shell and away from closed shell then reveal how the residual interaction is modified by the different core structures.

In the last few years, the structure of odd-odd Sb nuclei in 110 mass region have been experimentally investigated using heavy ion beams and large detector arrays [19–24]. One common characteristic of these odd-odd Sb nuclei is the presence of  $\Delta J=1$  rotational band with  $\Delta J=2$  crossover transitions and this band has a most likely configuration of  $\pi g_{9/2}^{-1} \pi g_{7/2}^2 \otimes \nu h_{11/2}$ . The high spin states of  $^{112}\text{Sb}$  have been studied through heavy ion fusion reactions [21,25]. Recently, low-lying states of  $^{112}\text{Sb}$  have been populated using  $^{112}\text{Sn}(p,n\gamma)^{112}\text{Sb}$  reaction [26]. A few new energy levels in the low energy region have been placed and the placement of some of the transitions has been changed in the new level scheme of  $^{112}\text{Sb}$ . Interacting Boson Fermion Fermion Model (IBFFM) was used to understand the low-lying structures of heavier odd-odd Sb nuclei [27–31] and nice systematics in energy splitting of proton-neutron multiplets have been obtained.

The aim of this work is to study both the low and the high spin structures of odd-odd  $^{112}\text{Sb}$  in the frame-

work of IBFFM. Magnetic moments of the ground state and the isomeric  $8^-$  state and E2/M1 mixing ratios( $\delta$ ) of some of the low-lying transitions have been calculated. The  $\beta$ -decay matrix elements for the Gamow-Teller transitions in  $^{112}\text{Sb} \rightarrow ^{112}\text{Sn}$  and  $^{111}\text{Sb} \rightarrow ^{111}\text{Sn}$  decay have also been calculated and are compared with the experimental values. The band based on the  $\pi g_{9/2}^{-1} \pi g_{7/2}^2 \otimes \nu h_{11/2}$  configuration has been reproduced. The B(M1)/B(E2) ratios for the transitions in this band have also been calculated and compared with the experimental values.

## 2 Theory

The Hamiltonian describing the odd-odd nuclei is

$$H = H_B + H_{B\pi} + H_{B\nu} + H_\pi + H_\nu + H_{\pi\nu} \quad (1)$$

where  $\pi$  ( $\nu$ ) refers to single proton (neutron) and B refers to the boson core. Here, the different terms represent the Hamiltonian for the boson core, boson-proton and boson-neutron interactions, fermion single particle interaction and proton-neutron residual interaction, respectively.

The boson part is the usual IBM-1 Hamiltonian [32]. The boson-fermion interaction, which describes the odd-mass nuclei, have the simple form given by [33,34]. A surface delta [35] plus spin-spin interaction has been taken as the residual interaction between the odd proton and the odd neutron.

$$H_{\pi\nu} = -A(1 - \alpha + \alpha \boldsymbol{\sigma}_\pi \cdot \boldsymbol{\sigma}_\nu) \delta(\mathbf{r}_\pi - \mathbf{r}_\nu) + V_{\sigma\sigma} \boldsymbol{\sigma}_\pi \cdot \boldsymbol{\sigma}_\nu \quad (2)$$

where A,  $\alpha$  and  $V_{\sigma\sigma}$  are adjustable parameters.

For the electromagnetic properties, the one body electromagnetic transition operator is taken to be of the form

$$T(\lambda) = T_B(\lambda) + T_F(\lambda) \quad (3)$$

where the first term operates on the boson part and the last term on the fermion part of the wave function.

The electromagnetic transition operators for the E2 and M1 transition for the bosons, respectively are

$$T_B(E2) = e_B[(s^\dagger \tilde{d} + d^\dagger \tilde{s})^2 + \chi(d^\dagger \tilde{d})^2] \quad (4)$$

and

$$T_B(M1) = g_d(d^\dagger \tilde{d})^1 + \eta[T_B(E2) \times \hat{L}]^1 \quad (5)$$

The corresponding E2 transition operator for the fermions is given by

$$T_F(E2) = \sum_{jj'} e_F \langle j || Y_2 || j' \rangle (a_j^\dagger \tilde{a}_{j'})^2. \quad (6)$$

The fermion operator for M1 transition is given in [36].

One of the powerful methods to test the models of nuclear structure is the evaluation of the  $\beta$ -decay matrix elements for the Gamow-Teller transitions. The beta decay rates are very sensitive to the details of the nuclear wave functions. Even small admixtures in the wavefunction can change the resulting  $ft$  value considerably. The operators

for the Gamow-Teller transitions between odd-even and even-odd and between odd-odd and even-even nuclei are described in [37].

The  $ft$  values can be obtained using the expression

$$ft = \frac{6163}{(G_A/G_V)^2 \langle M_{GT} \rangle^2} s \quad (7)$$

where  $M_{GT}$  denotes the matrix element of the Gamow-Teller operator and  $G_A$ ,  $G_V$  are the axial vector and vector coupling constants, respectively, whose ratio in free space is  $1.59 \pm 0.02$ . The value of this ratio adopted in this calculation is 1.2, a usual value used for the nuclei [38].

## 3 Calculation

This section has been divided into two parts describing the low spin and high spin structures in  $^{112}\text{Sb}$  separately.

### 3.1 The low lying levels

The low-lying structure of  $^{112}\text{Sb}$  can be understood in terms of quasiparticle excitations coupled to the vibrational levels of  $^{110}\text{Sn}$  core. Here, the even-even core consists of five neutron bosons above  $Z = N = 50$ . In this calculation, the core parameters are taken from our earlier calculation for  $^{112}\text{Sn}$  which treats the core as a anharmonic vibrator [8] and the same are used here for  $^{110}\text{Sn}$ . The values of the parameters used in the present calculation are given in Table 1. Here,  $\epsilon_d$  is the d-boson energy and  $C_L$  are the coefficients of the anharmonicity terms in the IBM-1 Hamiltonian [32].

In order to describe odd-odd nuclei in IBFFM, it is necessary to obtain the parameters which describe the odd-proton and the odd-neutron nuclei. The quasiparticle energies ( $\epsilon_j$ ) and the occupancy of the levels ( $v_j^2$ ) used for the description of odd-mass Sn and Sb nuclei in IBFM are obtained from a self-consistent BCS calculation with the pairing strength  $G_p = 0.2$  MeV for both type of particles in the available shell model space consisting of  $1g_{7/2}$ ,  $2d_{5/2}$ ,  $2d_{3/2}$ ,  $3s_{1/2}$  and  $1h_{11/2}$  single particle orbitals. The single particle energy values has been taken from [39]. The parameters  $A_0$ ,  $T_0$  and  $\Lambda_0$  are the coefficients of the monopole, quadrupole and exchange terms in the boson-fermion interaction [34]. The calculation has been done using the computer code ODDA [40]. The parameters used in the IBFM calculation are given in Table 1. The experimental energy values for  $^{111}\text{Sn}$  and  $^{111}\text{Sb}$  are taken from [9] and [13], respectively.

Using the above parameters, IBFFM calculation has been performed for  $^{112}\text{Sb}$ . The details of the method of calculation are given in ref. [41]. To restrict the number of basis states, the maximum number of d-bosons has been limited to three in this calculation. This truncation is good enough for the description of the low-lying states. The parameters  $A$ ,  $\alpha$  and  $V_{\sigma\sigma}$  in (2) are adjusted to get a good fit for the low lying energy levels.

**Table 1.** Parameters used in this calculation. All the parameters are in units of MeV except  $v_j^2$ ,  $\chi$  and  $\alpha$  which are dimensionless quantities

For low-lying states	$^{110}\text{Sn}$ core	$\epsilon_d$	1.2				
		$C_0$	-0.30				
		$C_2$	-0.15				
	$^{111}\text{Sn}$ $\nu$ sector	$A_0$	-0.079	$\epsilon_{5/2}$	1.480	$v_{5/2}^2$	0.803
		$\Gamma_0$	0.376	$\epsilon_{7/2}$	1.181	$v_{7/2}^2$	0.541
		$A_0$	0.476	$\epsilon_{3/2}$	2.238	$v_{3/2}^2$	0.075
				$\epsilon_{1/2}$	1.483	$v_{1/2}^2$	0.195
				$\epsilon_{11/2}$	1.989	$v_{11/2}^2$	0.097
	$^{111}\text{Sb}$ $\pi$ sector	$A_0$	0.130	$\epsilon_{5/2}$	0.821	$v_{5/2}^2$	0.100
		$\Gamma_0$	0.350	$\epsilon_{7/2}$	1.800	$v_{7/2}^2$	0.019
		$A_0$	-1.330	$\epsilon_{3/2}$	2.504	$v_{3/2}^2$	0.010
				$\epsilon_{1/2}$	2.848	$v_{1/2}^2$	0.008
				$\epsilon_{11/2}$	2.071	$v_{11/2}^2$	0.015
	$^{112}\text{Sb}$	A	-0.25				
$\alpha$		-0.05					
$V_{\sigma\sigma}$		-0.05					
For high spin states	$^{110}\text{Sn}$ core	$\epsilon_d$	0.6				
		$\kappa$	-0.167				
		$\chi_\nu$	-0.2				
		$\chi_\pi$	0.4				
		$C_{0\nu}$	0.0				
		$C_{2\nu}$	-0.06				
	$^{111}\text{Sn}$ $\nu$ sector	$A_0$	-0.147	$\epsilon_{11/2}$	0.0	$v_{11/2}^2$	0.097
		$\Gamma_0$	0.650				
		$A_0$	0.600				
	$^{111}\text{Sb}$ $\pi$ sector	$A_0$	0.100	$\epsilon_{9/2}$	0.0	$v_{9/2}^2$	0.9
		$\Gamma_0$	0.755				
		$A_0$	-3.500				
	$^{112}\text{Sb}$	A	-0.25				
		$\alpha$	-0.05				
$V_{\sigma\sigma}$		-0.05					

The electromagnetic transition probabilities for the transitions between the low-lying states have been calculated to verify the composition of the wavefunctions. The value of the parameters  $e_B$  and  $\chi$  used in the calculation are 9.0 and 0.7 respectively and are taken from an earlier work [8] for  $^{112}\text{Sn}$ . In the present case the fermionic charge  $e_F$  is taken equal to  $e_B$ . The g-factor for the bosons are calculated from the  $Z/A$  ratio which is 0.45 for the  $^{112}\text{Sb}$ . The parameter  $\eta$  is 1.0 in this calculation.

### 3.2 The high spin states

Recent experimental data [9–11] suggests the configuration of the rotational bands in Sn and Sb nuclei to be based on the high-j orbitals  $\nu h_{11/2}$  and  $\pi g_{9/2}$ . To study the rotational band in the odd-odd  $^{112}\text{Sb}$  in the IBFFM model, the following procedure has been employed.

The predicted configuration for the band in  $^{112}\text{Sb}$  is  $\pi g_{9/2}^{-1} \pi g_{7/2}^2 \otimes \nu h_{11/2}$  [21]. In IBFFM, the levels in this

band can be understood in terms of the odd proton (in  $g_{9/2}$ ) and the odd neutron (in  $h_{11/2}$ ) coupled to the 2p-2h band of the even-even  $^{110}\text{Sn}$  core. Since the lower members of 2p-2h band in  $^{110}\text{Sn}$  have not been observed, we have used the same parameters as in the description of the 2p-2h band in  $^{112}\text{Sn}$  [8]. Here, apart from the parameters already described in the previous subsection,  $\kappa$  refers to the coefficient of the proton-neutron quadrupole-quadrupole interaction term in the IBM-2 Hamiltonian [32]. For the calculation in odd and odd-odd nuclei, this Hamiltonian is projected on the IBM-1 space.

The deformed rotational band in  $^{111}\text{Sn}$  has the configuration  $(2p-2h) \otimes \nu h_{11/2}$ . IBFM parameters for this band of  $^{111}\text{Sn}$  have been obtained by fitting the experimental energy levels with the odd-neutron in the  $h_{11/2}$  orbital using the computer code ODDA. The occupation probability for the  $h_{11/2}$  orbital has been kept the same as used for the description of low-lying states. The three parameters used in the code  $A_0$ ,  $\Gamma_0$  and  $\Lambda_0$  are adjusted to reproduce the above band. The experimental values are taken from [9]. Similar calculation for the  $g_{9/2}$  band of  $^{111}\text{Sb}$  has been carried out keeping the odd proton in the  $g_{9/2}$  orbital. The occupancy for this orbital has been taken equal to 0.9. The number of bosons is seven in this case.

The coupled rotational band in  $^{112}\text{Sb}$  has been reproduced using the above parameters. For the residual interaction part, the same set of parameters as used in the calculation of level properties of low-lying levels, have been used. No truncation in the number of d-bosons has been made for this configuration.  $B(M1)/B(E2)$  ratios and branching ratios for the transitions in the above band have been calculated using the wave functions thus obtained. The effective d-boson charge is 12e and the parameter  $\chi$  is taken equal to zero.

## 4 Results and discussion

In the reported level schemes of  $^{112}\text{Sb}$  studied through heavy-ion reactions [21,25], there exist some contradictions regarding the placement of the 29 keV  $\gamma$ -transition. Singh *et al.* [21] have placed this  $\gamma$ -transition, which was unobserved in their experiment, above the previously known isomeric state with  $J^\pi=8^-$  at 796 keV and proposed a state with  $J^\pi=7^-$  at 825 keV to accommodate this transition. However, in a later study by Moon *et al.* [25], a 30 keV transition have been observed in coincidence with the 103 and 237 keV  $\gamma$ -rays. Therefore, they have placed this transition above the 103 keV state in their level scheme. As a result they propose the excitation energy of the isomeric state should be at 825 keV. Recently, low energy state of  $^{112}\text{Sb}$  has been populated through  $(p, n\gamma)$  reaction [26]. They also have obtained indirect evidences for the existences of a 26 keV transition above the 103 keV state. So if the placement of the 29 keV transition above 103 keV state is correct, the levels at 340 and 796 keV in the ref. [21] will be shifted by an amount 29 keV and this will inturn shift the  $8^-$  state to 825 keV. The data of Singh *et al.* [21] do not contradict the spin assignment of 7 to this state. The 1122 keV transition which

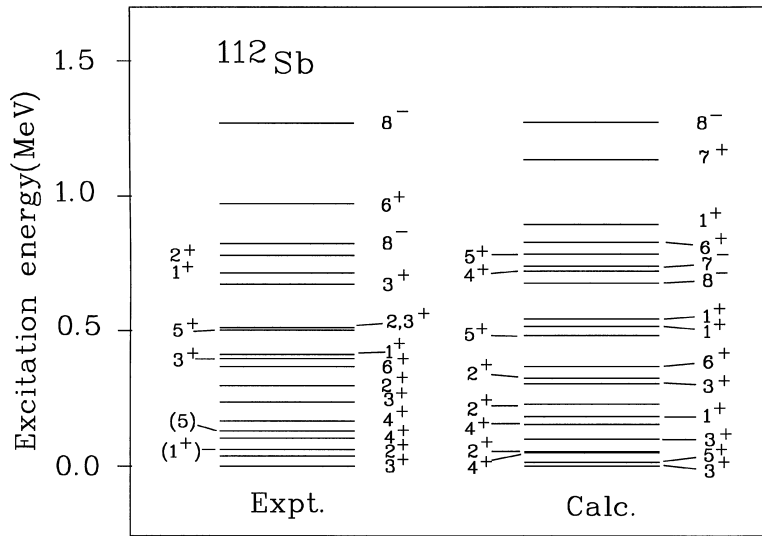


**Fig. 1.** Comparison of experimental and calculated low-lying energy levels of  $^{112}\text{Sb}$

decays to this level was assigned a quadrupole multipolarity. However, in view of the large error in this relatively weak transition, a dipole assignment can not be ruled out.

Another point of contradiction in the above two works [21,25] lies in the spin assignment for the states arising from  $\pi g_{9/2}^{-1} \pi g_{7/2}^2 \otimes \nu h_{11/2}$  configuration. In the ref. [25], a spin-parity  $9^-$  was assigned to the 1746 keV level of this band primarily based on the DCO ratio of the 1122 keV transition whereas Singh *et al.* [21] has assigned a spin-parity of  $8^-$  to the same, leading to a difference of one unit in the spin values of the other members of the band. It is to be mentioned that there should be a transition in the low energy region, which connects the positive parity low-lying states and this negative parity band. The 701 keV transition appears to be the only possible candidate connecting the negative and positive parity states. In the work of Moon *et al.* [25] this has been shown as a transition of multipolarity two whereas the DCO ratio measurement by Singh *et al.* [21] suggests that this is a stretched transition of multipolarity one. In view of this the spin-parity of the 1746 keV level should be  $8^-$ . Systematics of other odd-odd Sb isotopes [19,20,22,23] also suggest the spin assignment of  $8^-$  to this level. Therefore, in the present calculation, the spin assignment of the said band given in the [21] has been followed. The energy value and spin-parity assignment to low-lying state are mostly taken from [26].

The calculated and experimental energy values for the low lying states of  $^{112}\text{Sb}$  isotope are compared in Fig. 1. Experimental values are taken from [26,21]. Since the neutrons outside the  $N = 50$ ,  $^{100}\text{Sn}$  core in  $^{112}\text{Sb}$  occupy mainly  $\nu g_{7/2}$  and  $\nu d_{5/2}$  orbital, the most of the low lying states in  $^{112}\text{Sb}$  are expected from  $\pi d_{5/2} \otimes \nu g_{7/2}$  and  $\pi d_{5/2} \otimes \nu d_{5/2}$  configurations coupled to the  $n_d = 0$  state of the core. The ground state spin  $3^+$  of  $^{112}\text{Sb}$  is correctly reproduced and has a major contribution from the  $\pi d_{5/2} \otimes \nu g_{7/2}$  configuration in its wavefunction. The first  $5^+$ ,  $2^+$ ,  $4^+$ ,  $1^+$  and  $6^+$  are the other multiplets of this configuration. The dominant wave function components and

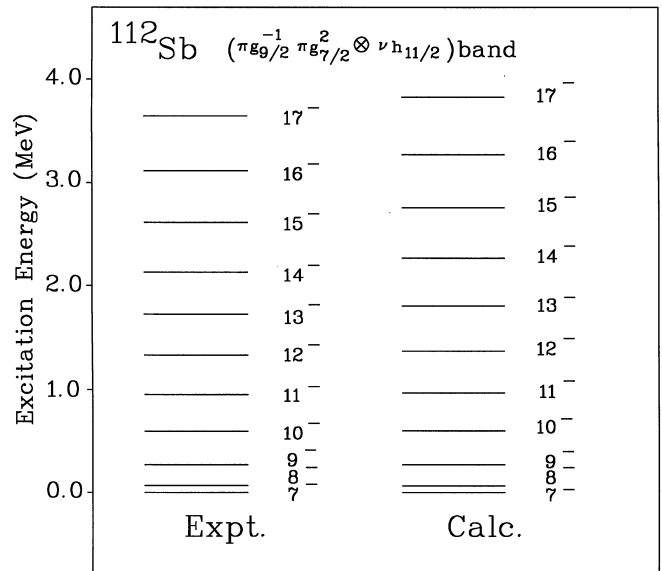


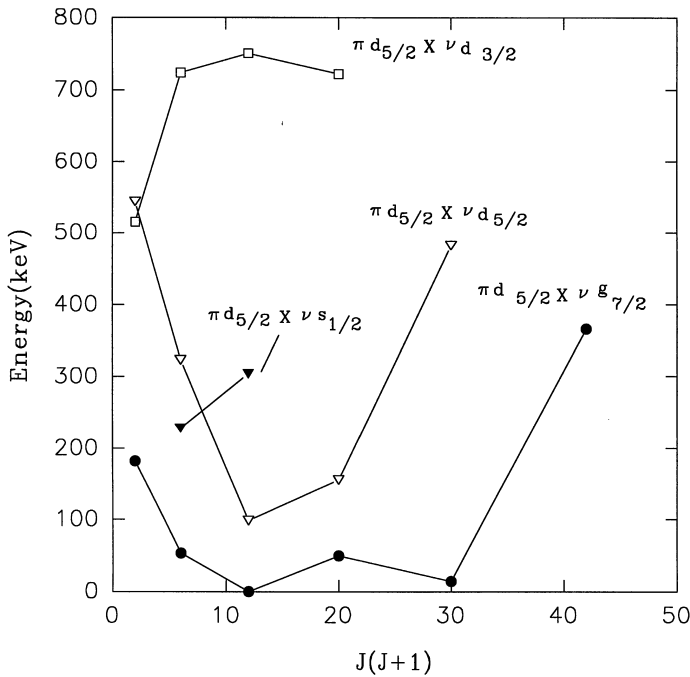
**Fig. 2.** Comparison of experimental and calculated energy levels belonging to the configuration  $\pi g_{9/2}^{-1} \pi g_{7/2}^2 \otimes \nu h_{11/2}$  of  $^{112}\text{Sb}$

corresponding amplitudes of few low-lying states are given in Table 2. The calculated energy values of the multiplets of  $\pi d_{5/2} \nu g_{7/2}$ ,  $\pi d_{5/2} \nu d_{5/2}$ ,  $\pi d_{5/2} \nu s_{1/2}$  and  $\pi d_{5/2} \nu d_{3/2}$  proton neutron combination are plotted against  $J(J+1)$  in Fig. 3. It is clear from Fig. 3 that the parabolic feature [42] of the multiplets of different proton neutron combinations is approximately reproduced by this calculation.

The negative parity states in the low energy region arise due to motion of particle, proton or neutron, in the  $h_{11/2}$  orbital. The calculated energy of the  $8^-$  state, which is the lowest among the negative parity states in this calculation, agree with the experimental observation. The first  $8^-$  state originates due to neutron motion in  $h_{11/2}$  orbital and is the multiplet of the  $\pi d_{5/2} \otimes \nu h_{11/2}$  configuration whereas the second  $8^-$  state is the proton counter-

**Table 2.** Wave-function of few low-lying states of  $^{112}\text{Sb}$ . For the given  $J^\pi$  state the  $[[j_\pi(j_\nu|n_dL)]I]J$  wave-function components and the corresponding amplitudes are given

$J^\pi$	W.f. comp.	Amplitudes	$J^\pi$	W.f. comp.	Amplitudes
$1_1^+$	$\frac{5}{2}(\frac{7}{2};00)$	0.859	$4_2^+$	$\frac{5}{2}(\frac{5}{2};00)$	0.836
$1_2^+$	$\frac{5}{2}(\frac{5}{2};00)$	0.638	$4_3^+$	$\frac{5}{2}(\frac{3}{2};00)$	-0.597
	$\frac{5}{2}(\frac{3}{2};00)$	0.522		$\frac{5}{2}(\frac{7}{2};00)$	0.457
$1_3^+$	$\frac{5}{2}(\frac{5}{2};00)$	-0.610	$5_1^+$	$\frac{5}{2}(\frac{7}{2};00)$	0.917
	$\frac{5}{2}(\frac{3}{2};00)$	0.361			
$1_4^+$	$\frac{7}{2}(\frac{7}{2};00)$	-0.511	$5_2^+$	$\frac{5}{2}(\frac{5}{2};00)$	0.857
	$\frac{7}{2}(\frac{5}{2};12)$	0.446			
$2_1^+$	$\frac{7}{2}(\frac{7}{2};00)$	0.865	$5_3^+$	$\frac{7}{2}(\frac{7}{2};00)$	-0.684
				$\frac{7}{2}(\frac{5}{2};00)$	-0.329
$2_2^+$	$\frac{5}{2}(\frac{1}{2};00)$	-0.618	$6_1^+$	$\frac{5}{2}(\frac{7}{2};00)$	-0.889
	$\frac{5}{2}(\frac{3}{2};00)$	-0.507			
$2_3^+$	$\frac{5}{2}(\frac{5}{2};00)$	-0.684	$6_2^+$	$\frac{7}{2}(\frac{7}{2};00)$	0.825
	$\frac{5}{2}(\frac{3}{2};00)$	0.410			
$2_4^+$	$\frac{3}{2}(\frac{3}{2};00)$	0.572	$7_1^+$	$\frac{7}{2}(\frac{7}{2};00)$	0.756
	$\frac{7}{2}(\frac{7}{2};12)$	0.440		$\frac{5}{2}(\frac{7}{2};12)$	0.459
$3_1^+$	$\frac{5}{2}(\frac{7}{2};00)$	0.887	$7_1^-$	$\frac{5}{2}(\frac{11}{2};00)$	-0.878
$3_2^+$	$\frac{5}{2}(\frac{5}{2};00)$	0.624	$7_2^-$	$\frac{11}{2}(\frac{7}{2};00)$	0.626
	$\frac{5}{2}(\frac{3}{2};00)$	0.602		$\frac{11}{2}(\frac{5}{2};00)$	0.629
$3_3^+$	$\frac{5}{2}(\frac{5}{2};00)$	-0.505	$8_1^-$	$\frac{5}{2}(\frac{11}{2};00)$	0.782
	$\frac{5}{2}(\frac{3}{2};00)$	0.562		$\frac{5}{2}(\frac{11}{2};12)$	-0.400
$3_4^+$	$\frac{3}{2}(\frac{3}{2};00)$	0.635	$8_2^-$	$\frac{11}{2}(\frac{7}{2};00)$	-0.909
	$\frac{7}{2}(\frac{5}{2};12)$	0.474			
$4_1^+$	$\frac{7}{2}(\frac{7}{2};00)$	-0.852			

**Fig. 3.** Calculated energy versus  $J(J+1)$  plot for the states of different proton-neutron multiplets**Table 3.** Comparison of experimental and calculated mixing ratio  $\delta$  of the transitions in  $^{112}\text{Sb}$ 

initial level		Final level		$E_\gamma$ keV	$\delta$ Exp.	$ \delta $ Calc.
$J^\pi$	keV	$J^\pi$	keV			
$4_1^+$	104	$3_1^+$	0	104	-0.01(4)	0.005
$4_2^+$	167	$3_1^+$	0	167	+0.01(4)	0.005
$3_2^+$	236	$4_2^+$	167	69	+0.02(8)	0.007
		$4_1^+$	104	133	-0.07(6)	0.015
		$2_1^+$	38	198	-0.04(6)	0.003
$2_2^+$	296	$3_1^+$	0	296	-0.07(4)	0.03
$3_3^+$	396	$2_1^+$	38	357	+0.01(5)	0.009
		$4_1^+$	104	292	+0.07(9)	0.03
$1_2^+$	411	$2_1^+$	38	373	-0.07(4)	0.06
$5_2^+$	502	$4_1^+$	104	398	-0.14(8)	0.04
		$4_2^+$	167	335	-0.14(8)	0.04
$1_3^+$	714	$2_2^+$	296	418	+0.28(56)	0.004

part and has major contribution from  $\pi h_{11/2} \otimes \nu d_{5/2}$  to its wavefunction.

The negative parity states arising from the coupling of proton and neutron to the  $2^+$  i.e.  $n_d=1$  state of the  $^{110}\text{Sn}$  vibrational core are expected around 1700 keV of energy. In the experimental energy spectrum no such state has been observed.

The calculated values of the magnetic moment of the ground state and the  $8^-$  isomeric state at 825 keV are  $1.528 \mu_N$  and  $2.592 \mu_N$ , respectively. The corresponding experimental value for  $8^-$  state is  $2.20 \mu_N$  [43]. No data on magnetic moment for the ground state of  $^{112}\text{Sb}$  is available. So experimental determination would be an useful additional test of the theoretical interpretation. The good agreement between the experimental and the calculated values confirms the predicted configuration of this  $8^-$  state. The E2/M1 mixing ratios( $\delta$ ) have been calculated for some of the low-lying states and are compared in Table 3 with the experimental values. In a majority of the cases the calculated mixing ratios agree with the experimental ones within the error limits. The experimental values are taken from [26].

Beta decay rates for the Gamow-Teller transitions have also been calculated for both odd-odd to even-even and odd-even to even-odd nuclei. The calculated and experimental  $\log ft$  values are compared in Table 4. A reasonably good agreement between the calculated and the experimental values have been obtained for all transitions, ex-

**Table 4.** Beta decay rates for the transitions between  $^{112}\text{Sb} \rightarrow ^{112}\text{Sn}$  and  $^{111}\text{Sb} \rightarrow ^{111}\text{Sn}$  nuclei

Initial nucleus	$J^\pi$	Final nucleus	$J^\pi$	Energy (keV)	$\log ft$ expt.	$\log ft$ calc.
$^{112}\text{Sb}$	$3^+$	$^{112}\text{Sn}$	$2^+$	1256	5.1	5.0
			$4^+$	2248	5.4	7.9
$^{111}\text{Sb}$	$\frac{5}{2}^+$	$^{111}\text{Sn}$	$\frac{3}{2}^+$	643	4.7	4.4
			$\frac{3}{2}^+$	1032	4.7	5.0

**Table 5.** Comparison of the calculated and the experimental  $B(M1)/B(E2)$  ratios of the  $\gamma$ -transitions and branching ratios of the energy levels in the band. The numbers in the parenthesis represent errors in the corresponding experimental values

$B(M1)/B(E2)$ ratio in $\mu_N^2/e^2b^2$			Branching ratio in %						
$\frac{(J \rightarrow J-1)}{(J \rightarrow J-2)}$	Expt.	Calc.	$J_i$	energy (keV)	$J_f$	energy (keV)	$E_\gamma$ (keV)	Expt.	Calc.
$\frac{(10^- \rightarrow 9^-)}{(10^- \rightarrow 8^-)}$	10.8(1.6)	31.1	$10^-$	2273	$8^-$	1746	528	10	3
					$9^-$	1948	325	90	97
$\frac{(11^- \rightarrow 10^-)}{(11^- \rightarrow 9^-)}$	11.3(1.3)	14.1	$11^-$	2626	$9^-$	1948	678	18	14
					$10^-$	2273	353	82	86
$\frac{(12^- \rightarrow 11^-)}{(12^- \rightarrow 10^-)}$	12.5(1.5)	15.0	$12^-$	3006	$10^-$	2273	733	16	16
					$11^-$	2626	380	84	84
$\frac{(13^- \rightarrow 12^-)}{(13^- \rightarrow 11^-)}$	13.0(2.2)	11.5	$13^-$	3398	$11^-$	2626	772	18	22
					$12^-$	3006	392	82	78
					$13^-$	3380	426	31	0
$\frac{(14^- \rightarrow 13^-)}{(14^- \rightarrow 12^-)}$	7.8(1.2)	11.8	$14^-$	3805	$12^-$	3006	799	29	23
					$13^-$	3398	406	40	77
					$13^-$	3380	426	31	0
$\frac{(15^- \rightarrow 14^-)}{(15^- \rightarrow 13^-)}$	19.5(4.0)	9.8	$15^-$	4291	$13^-$	3398	893	21	26
					$14^-$	3805	486	79	74
$\frac{(16^- \rightarrow 15^-)}{(16^- \rightarrow 14^-)}$	13.3(6.4)	11.2	$16^-$	4793	$14^-$	3805	988	49	32
					$15^-$	4291	502	51	68
$\frac{(17^- \rightarrow 16^-)}{(17^- \rightarrow 15^-)}$	11.6(3.0)	9.4	$17^-$	5321	$15^-$	4291	1031		37
					$16^-$	4793	528		63

cept the one between the  $3^+$  state of  $^{112}\text{Sb}$  and the  $4^+$  state of  $^{112}\text{Sn}$ . The possible reason for this deviation is the assumption that the  $4^+$  state is a pure vibrator state. Theoretical calculation also shows that the wavefunction of first  $4^+$  state in all even-even Sn isotopes has a sizable contribution from the deformed rotational band based on (2p-2h) configuration [8].

The calculated and the experimental energy spectra for the  $\pi g_{9/2}^{-1} \pi g_{7/2}^2 \otimes \nu h_{11/2}$  band of  $^{112}\text{Sb}$  are compared in Fig. 2. This calculation predicts the  $7^-$  state as the band head for the band based on the above configuration. The calculated energy difference between the  $8^-$  and  $7^-$  is 66 keV suggesting that the observed 72 keV transition is also a member of this band. Similar conclusion has also been drawn for the 91 keV transition in  $^{108}\text{Sb}$  by Cederkäll *et al.* [19] on the basis of its angular distribution ratio. The overall agreement between the calculated and the experimental energy spectra is quite good. However, the sudden increase in the spacing at spin  $14^-$  can not be explained by this model. This may be due to interaction with another band, crossing around this spin value [21]. The dip in experimentally observed  $B(M1)/B(E2)$  ratio [21] also indicates the mixed nature of the states around  $14^-$  spin. The other possible configurations giving rise to a negative parity band are either  $\pi(g_{7/2}$  or  $d_{5/2}) \otimes \nu h_{11/2}$  or  $\pi h_{11/2} \otimes \nu(g_{7/2}$  or  $d_{5/2})$ . However, no band based on  $g_{7/2}$  orbital has been observed in the  $^{111}\text{Sb}$  and  $^{111}\text{Sn}$ .

The  $B(M1)/B(E2)$  ratios for the transitions in the above mentioned band have also been calculated. The calculated ratios (Table 5) have a decreasing trend with in-

creasing spin value, which is not in agreement with the experimental observation. The theoretical result is not unexpected, since the band becomes more and more deformed with increasing spin resulting in an enhancement in the  $B(E2)$  values of the transitions. The discrepancies in the low spin region indicates some other contributions to these states [21]. This calculation also predicts a number of negative parity states around 1.7 MeV which arise from coupling of odd-proton and odd-neutron to  $2^+$  state of the core. So, there is a high probability of mixing between these quasiparticle states and the above mentioned band structure. The agreement is better for the higher energy levels. The calculated M1 and E2 branching ratios for the transitions from the different states of the band are compared with the experimental results in Table 5. The enhancement in the E2 transition strength with increasing spin value is well reproduced by this calculation. However, the branching from the  $14^-$  state can not be explained by this model. The second  $13^-$  state at 3380 keV is possibly outside the present model space.

## 5 Summary

The structure of the low and the high spin states of odd-odd  $^{112}\text{Sb}$  has been investigated using the formalisms of Interacting Boson Fermion Fermion Model. Surface delta, spin delta and spin-spin type of interactions have been used to describe the residual interaction between the odd proton and the odd neutron. Energy levels, magnetic moments of the ground state and the isomeric  $8^-$  state,

E2/M1 mixing ratios of some of the low-lying transitions and  $\log ft$  values for the Gamow-Teller transitions in  $^{112}\text{Sb} \rightarrow ^{112}\text{Sn}$  and  $^{111}\text{Sb} \rightarrow ^{111}\text{Sn}$  decay have been obtained using this simplified model. The overall agreement between the value of calculated and experimental observables is quite satisfactory. Energy levels of  $\pi g_{9/2}^{-1} \pi g_{7/2}^2 \otimes \nu h_{11/2}$  band have been reproduced well in this calculation by coupling the proton (in  $g_{9/2}$ ) and the neutron (in  $h_{11/2}$ ) to the 2p-2h band of the  $^{110}\text{Sn}$ . However, the decay modes of the band members are not fully understood in this model. The experimental data indicate that the wavefunction of the states in the band have significant contribution from a band of somewhat different origin. The contribution from the spherical states may also influence the decay pattern. A more complete description of the high spin states therefore requires inclusion of both spherical and deformed configurations together in the model space.

The calculations were done using the computer facilities provided by the D.S.A. Programme of the Department of Physics, University of Calcutta. The author acknowledges G. Gangopadhyay, R. Bhattacharya and D. Banerjee for stimulating discussions and making helpful comments. He also wants to thank S. Bhattacharya of Saha Institute of Nuclear Physics, Calcutta for helpful discussions. The author also wishes to thank the University Grants Commission, New Delhi, for financial support.

## References

1. A. Bohr and B. R. Mottelson, Nuclear structure, vol 2, Benjamin, New York (1975)
2. S. Sen, B. K. Sinha, Nucl. Phys. **A157**, 497 (1970)
3. G. VandenBerghe, K. Heyde, Nucl. Phys. **A163**, 478 (1971)
4. J. Bron, *et al.*, Nucl. Phys. **A318**, 335 (1979)
5. D. Viggars, H. W. Taylor, B. Singh, J. C. Waddington, Phys. Rev. **C36**, 1006 (1987)
6. R. Wadsworth, *et al.*, Nucl. Phys. **A559**, 461 (1993)
7. R. Wadsworth, *et al.*, Phys. Rev. **C50**, 483 (1994)
8. A. K. Singh, G. Gangopadhyay, D. Banerjee, Phys. Rev. **C55**, 968 (1997)
9. G. Gangopadhyay, *et al.*, Z. Phys. **A351**, 1 (1995)
10. D. R. LaFosse, *et al.*, Phys. Rev. **C51**, R2876 (1995)
11. V. P. Janzen, *et al.*, Phys. Rev. Lett. **72**, 1160 (1994)
12. H. Schnare, *et al.*, Phys. Rev. **C54**, 1598 (1996)
13. D. R. LaFosse, *et al.*, Phys. Rev. **C50**, 1819 (1994)
14. V. P. Janzen, *et al.*, Phys. Rev. Lett. **70**, 1065 (1993)
15. V. P. Janzen, Phys. Scr. **T56**, 144 (1995)
16. C. -B. Moon, S. J. Chae, J. H. Ha, T. Komatsubara, J. Lu, T. Hayakawa, K. Furuno, Z. Phys. **A352**, 245 (1995)
17. R. S. Chakravarthy, R. G. Pillay, Phys. Rev. **C54**, 2319 (1996)
18. D. R. LaFosse, *et al.*, Phys. Rev. Lett. **69**, 1332 (1992)
19. R. Cederkäll, *et al.*, Nucl. Phys. **A581**, 189 (1995)
20. G. J. Lane, *et al.*, Phys. Rev. **C55**, R2127 (1997)
21. A. K. Singh, *et al.*, Nucl. Phys. **A607**, 350 (1996)
22. P. Van Nes, W. H. A. Hesselink, W. H. Dickhoff, J. J. Van Ruyven, M. J. A. DeVoigt, H. Verheul, Nucl. Phys. **A379**, 35 (1982)
23. R. Duffait, *et al.*, Z. Phys. **A307**, 259 (1982)
24. E. S. Paul, *et al.*, Phys. Rev. **C50**, 2297 (1994)
25. C. -B Moon, J. U. Kwon, T. Komatsubara, T. Saitoh, N. Hashimoto, J. Lu, H. Kimura, T. Hayakawa, K. Furuno, Z. Phys. **A357**, 5 (1997)
26. M. Fayez-Hassan, J. Gulyás, Zs. Dombrádi, I. Dankó, Z. Gácsi, Phys. Rev. **C55**, 2244 (1997)
27. Z. Gácsi, Zs. Dombrádi, T. Fényes, S. Brant, V. Paar, Phys. Rev. **C44**, 642 (1991)
28. M. Gulyás, T. Fényes, M. Fayez, F. M. Hassan, Zs. Dombrádi, J. Kumpulainen and R. Julin, Phys. Rev. **C46**, 1218 (1992)
29. T. Fényes, Zs. Dombrádi, Phys. Lett. **275B**, 7 (1992)
30. T. Fényes, Zs. Dombrádi, Z. Gácsi, J. Gulyás, Acta. Phys. Acad. Sci. Hung. **71**, 239 (1992)
31. Zs. Dombrádi, T. Fényes, Z. Gácsi, J. Gulyás, S. Brant, V. Paar, in *Perspectives for the Interacting Boson Model*, edited by R.F. Casten *et al.* (World Scientific, Singapore 1994)
32. D. Bonatsos, *Interacting Boson Models of Nuclear Structure*, (Clarendon, Oxford 1988)
33. F. Iachello, O. Scholten, Phys. Rev. Lett. **43**, 679 (1979)
34. O. Scholten, Ph.D. Thesis, University of Groningen 1980
35. K. L. G. Heyde, *The Nuclear Shell Model*, (Springer-Verlag 1990)
36. O. Scholten, in *Progress in particle and nuclear physics*, edited by A. Faessler, (Pergamon, Oxford 1985), Vol. 14, p. 189
37. A. K. Singh, G. Gangopadhyay, Phys. Rev. **C55**, 2734 (1997)
38. F. Dellagiacomma, F. Iachello, Phys. Lett. **B218**, 399 (1989)
39. B. Reehal, R. Sorensen, Phys. Rev. **C2**, 819 (1970)
40. O. Scholten, The programme package ODDA, (unpublished)
41. A. K. Singh, G. Gangopadhyay, Phys. Rev. **C55**, 726 (1997)
42. V. Paar, Nucl. Phys. **A331**, 16 (1979)
43. D. De Frenne, E. Jacobs, Nucl. Data Sheets **79**, 639 (1996)